INTERNATIONAL JOURNAL OF
NUMERICAL ANALYSIS AND MODELING
Volume 19, Number 2-3, Pages 255–274

OPTIMAL CONTROL PROBLEM OF AN SIR MODEL WITH RANDOM INPUTS BASED ON A GENERALIZED POLYNOMIAL CHAOS APPROACH

YOON-GU HWANG, HEE-DAE KWON, AND JEEHYUN LEE

Abstract. This paper studies the optimal control problem of a susceptibleinfectiousrecovered (SIR) epidemic model with random inputs. We prove the existence and uniqueness of a solution to the SIR random differential equation (RDE) model and investigate the numerical solution to the model by using a generalized polynomial chaos (gPC) approach. We formulate the optimal control problem of the SIR RDE model and consider the gPC Galerkin method to convert the problem into an optimal control problem with high-dimensional ordinary differential equations. Numerical simulations show that to effectively control an epidemic, vaccination should be given at the highest rate in the first few days, and after that, vaccination should be stopped completely. In addition, we observe that the optimal control function and the corresponding states are very robust to the uncertainty of random inputs.

Key words. Optimal control problem, random differential equation, generalized polynomial chaos.

1. Introduction

Mathematical models can help predict the dynamics of disease transmission and evaluate the impact of control measures. The susceptible-infectious-recovered (SIR) model proposed by O. Kermack and A. G. McKendrick in 1927 [18] is a simple deterministic model to describe an epidemic. The model divides the host population into three compartments: susceptible (S), infectious (I), and recovered (R) individuals. Several studies have conducted outstanding surveys of basic compartment models and explored key features of modified models [2, 7, 14].

However, real-world problems often involve uncertainty due to a lack of information or measurement errors in the data, for example. The randomness in probability theory is used to express uncertainty, and stochastic models have been developed to better describe a complex phenomenon. The stochastic differential equation (SDE) and the random differential equation (RDE) are known to be effective tools in epidemiology. The SDE adds white noise to incorporate perturbation, and Ito integration is the key technique for the analysis [12, 19, 25, 26, 27]. Random variables are employed to represent uncertain input, including parameters and initial conditions, and the RDE is introduced as a result. In this research, we consider a random differential equation for the SIR model [3, 31].

There are analytical and numerical approaches to figure out the property of a solution to RDE models. The analytical one finds the probability density function of a solution by using random variable transformation [8, 17, 28, 30]. Among many numerical schemes to solve RDE models, Monte-Carlo simulation is the basic algorithm to characterize the solution. Generalized polynomial chaos (gPC) [9, 32] and the stochastic collocation method [32, 33] are useful choices in particular settings.

Received by the editors August 28, 2021 and, in revised form, November 26, 2021.
2000 *Mathematics Subject Classification.* 34F05, 49K15, 92B05.

Vaccination is one of the crucial interventions for reducing the spread of infectious diseases. In order to minimize disease burdens, it is important to determine the optimal vaccination policies to better allocate limited resources. Previous studies applied optimal control techniques to derive an efficient vaccination strategy for influenza outbreaks under specific circumstances [20, 21, 22, 23, 24, 34]. Lahrouz et al. considered two types of control to reduce the number of infectious individuals: treatment and preventive campaigns to avoid relapses [20]. Modified models were introduced to incorporate seasonal forcing and age-structure, and optimal strategies for vaccination, antiviral treatments, and social distancing were suggested in [21]. Li et al. proposed a model based on complex networks to discuss an effective quarantine scheme [24] and others have investigated the distribution of vaccines under limited resources using a model with group mixing [34]. Many researchers have also applied control theory to develop optimal strategies for other diseases including HIV, tuberculosis, and vector-borne diseases [1, 5, 15, 16].

The goal of this paper is to derive an optimal vaccination strategy using the SIR model with random inputs. To achieve that, the gPC Galerkin method, which can be applied to various numerical techniques and control theory, is employed. In Section 2, we formulate the SIR RDE model with a random transmission rate and initial conditions for a susceptible population. Then, the existence and uniqueness of a solution to the model are analyzed. A brief introduction to gPC in Section 3 is followed by applying the stochastic Galerkin method using an orthogonal polynomial basis to approximate a solution to the RDE model in Section 4. We also compare the gPC Galerkin solution with Monte-Carlo simulation to evaluate the quality of approximation. In Section 5, we explore an optimal control problem that minimizes the number of infected individuals while considering intervention costs. Finally, Section 6 presents the results from numerical simulations with several distributions of random variables, and we conclude with a summary in Section 7.

2. The SIR model with random inputs

In this section, we introduce an SIR model with random coefficients, and we prove the existence and uniqueness of a solution to the model equation. The SIR model consists of three compartments. The susceptible compartment, S, represents individuals who are susceptible to the disease, while the infectious compartment, I, represents infected individuals who can infect susceptible people. The recovered compartment, R, represents individuals who have recovered from the disease or who have been immunized against the disease. The SIR model with random inputs is given by the following random differential equation [3, 30, 31]:

$$\begin{cases} \dot{S}(t) &= -\beta S(t)I(t) - \mu u(t)S(t) \\ \dot{I}(t) &= \beta S(t)I(t) - \gamma I(t) \\ \dot{R}(t) &= \mu u(t)S(t) + \gamma I(t) \end{cases} \tag{1}$$

with initial conditions $S(0) = S_0, I(0) = I_0$ and $R(0) = R_0$.

The positive parameter β denotes the transmission rate of the disease, and μ is vaccination efficacy. Infected individuals leave infectious class I at rate γ. μ and γ are positive constants. The control function $u(t)$ indicates the rate at which susceptible individuals are vaccinated, and its value is assumed to be in the range $[0, 1]$. Usually, the parameters and initial conditions are considered to be constants in the deterministic model. In this paper, it is assumed that infection rate β and the initial value of susceptible compartment S_0 are functions of random variables

to express the uncertainty occurring in reality. Since state R is decoupled from the system of S and I, from now on we only consider the first two equations in (1) as follows:

$$\begin{cases} \dot{S}(t) &= -\beta(z)S(t)I(t) - \mu u(t)S(t) \\ \dot{I}(t) &= \beta(z)S(t)I(t) - \gamma I(t) \end{cases} \tag{2}$$

with initial conditions $S(0) = S_0(z)$ and $I(0) = I_0$.

To represent the uncertainty in transmission rate β and initial condition S_0, these values are assumed to be functions of random variable $z = (z_1, z_2) \in \mathbf{R}^2$ in the forms

$$\beta(z) = \beta_0 + \sigma_\beta \cdot z_1$$

and

$$S_0(z) = S_{0,0} + \sigma_{S_0} \cdot z_2$$

where β_0, σ_β, $S_{0,0}$, and σ_{S_0} are positive constants. Random variables z_1 and z_2 are assumed to be independent and identical distributed (i.i.d). Since model (2) is not deterministic, the model is not solvable numerically by a simple ODE solver. Monte Carlo simulation is a general method for numerically solving the RDE. In this paper, however, we consider gPC to solve RDE (2), and we further explore the optimal control problem with the RDE as the constraint equation. Throughout our paper, we denote that $(\Omega, \mathcal{F}, \mathbf{P})$ is a probability space. For random vector $z = (z_1, z_2, \cdots, z_n) \in \mathbf{R}^n$ in which the elements are mutually independent, we define $L^2_{\mathbf{P}}$ as follows:

$$z \in L^2_{\mathbf{P}}(\Omega) = \left\{ z \in \mathbf{R}^n \;\middle|\; \mathbf{E}[z^2] < \infty \right\}, \tag{3}$$

where $\mathbf{E}[\cdot] = \int_\Omega \cdot \, d\mathbf{P}(z) = \int_\Omega \cdot \, \rho(z)dz$ with the given probability density function $\rho(z)$.

2.1. Existence and Uniqueness. In this subsection, we first prove that there exists a unique solution to RDE (2). To achieve this, we use the following theorem (see [26] and [27]).

Theorem 2.1. *Let B_t be a Brownian motion. Consider a stochastic differential equation*

$$d\boldsymbol{x} = \boldsymbol{g}(t, \boldsymbol{x}) \; dt + \boldsymbol{\sigma}(t, \boldsymbol{x}) \; dB_t, \qquad \forall t \in [0, T] \tag{4}$$

where $\boldsymbol{x}(0) = \boldsymbol{x}_0$ is a random initial condition with $\boldsymbol{x}_0 \in L^2_{\mathbf{P}}(\Omega)$.

Assume that

$$||\boldsymbol{g}(t, \boldsymbol{x})||_2 + ||\boldsymbol{\sigma}(t, \boldsymbol{x})||_2 < C(1 + ||\boldsymbol{x}||_2), \qquad \forall \boldsymbol{x} \in \mathbf{R}^n, \tag{5}$$

and

$$||\boldsymbol{g}(t, \boldsymbol{x}) - \boldsymbol{g}(t, \boldsymbol{y})||_2 + ||\boldsymbol{\sigma}(t, \boldsymbol{x}) - \boldsymbol{\sigma}(t, \boldsymbol{y})||_2 < D||\boldsymbol{x} - \boldsymbol{y}||_2, \qquad \forall \boldsymbol{x}, \boldsymbol{y} \in \mathbf{R}^n, \tag{6}$$

where C and D are constants. Then (4) has a unique t-continuous solution $\boldsymbol{x}$ satisfying

$$\mathbf{E}\left[\int_0^T |\boldsymbol{x}|^2 \; dt \right] < \infty. \tag{7}$$

Here, $|| \cdot ||_2$ is the the L_2 norm on n-dimensional Euclidean space $\mathbf{R}^n$. The existence and uniqueness of the solution to (2) can now be demonstrated in the following theorem.

Theorem 2.2. *Assume that* $0 < \beta(z) < \beta_{max}$ *and* $0 < S_0(z) < S_{0,max}$. *Then, there is a unique solution to RDE* (2).

Proof. Let

$$\tilde{\boldsymbol{x}} = \begin{bmatrix} S \\ I \end{bmatrix} \quad \text{and} \quad \tilde{\boldsymbol{g}}(t, \tilde{\boldsymbol{x}}) = \begin{bmatrix} -\beta(z)SI - \mu u S \\ \beta(z)SI - \gamma I \end{bmatrix}.$$

With this notation, model equation (2) can be rewritten as

$$d\tilde{\boldsymbol{x}} = \tilde{\boldsymbol{g}}dt, \quad \text{with} \quad \tilde{\boldsymbol{x}}(0) = \tilde{\boldsymbol{x}}_0.$$

Here, $\tilde{\boldsymbol{\sigma}}(t, \tilde{\boldsymbol{x}}) = 0$.

Let

$$\boldsymbol{x} = \begin{bmatrix} S & I & \beta(z) \end{bmatrix}^T, \quad \boldsymbol{g} = \begin{bmatrix} \tilde{\boldsymbol{g}} & 0 \end{bmatrix}^T, \quad \text{and} \quad \boldsymbol{\sigma} = \begin{bmatrix} \tilde{\boldsymbol{\sigma}} & 0 \end{bmatrix}^T.$$

Then we obtain an augmented system to which Theorem 2.1 can be applied as follows:

$$d\boldsymbol{x} = \boldsymbol{g}(t, \boldsymbol{x})dt + \boldsymbol{\sigma}(t, \boldsymbol{x})\ dB_t, \tag{8}$$

where $x(0) = \begin{bmatrix} S(0) & I(0) & \beta(z) \end{bmatrix}^T$ and $\boldsymbol{\sigma}(t, \boldsymbol{x}) = 0$.

Since $\beta(z) < \beta_{max}$ and $S(t), I(t) < N_{tot}$ where N_{tot} denotes the total population, we have

$$||\boldsymbol{g}(t, \boldsymbol{x})||_2 = ||\tilde{\boldsymbol{g}}(t, \tilde{\boldsymbol{x}})||_2 = \left|\left| \begin{bmatrix} -\beta(z)SI - \mu u S \\ \beta(z)SI - \gamma I \end{bmatrix} \right|\right|_2 \leq C(1 + ||\tilde{\boldsymbol{x}}||_2) \leq C(1 + ||\boldsymbol{x}||_2).$$

That is, our stochastic differential equation (8) satisfies condition (5).

To show condition (6), we consider the gradient of $\boldsymbol{g}$:

$$\nabla \boldsymbol{g} = \begin{bmatrix} -\beta(z)I - \mu u & -\beta(z)S & -SI \\ \beta(z)I & \beta(z)S - \gamma & SI \\ 0 & 0 & 0 \end{bmatrix}.$$

It is clear that $|\nabla \boldsymbol{g}|$ is bounded due to the boundedness of $\beta(z)$, S, I, and u. So, $\boldsymbol{g}(t, \boldsymbol{x})$ is globally Lipschitz continuous with respect to $\boldsymbol{x}$, i.e., condition (6) is satisfied. Therefore, there exists a unique t-continuous solution to RDE SIR model (2) by Theorem 2.1. □

3. The generalized polynomial chaos approach

In this section, we apply the gPC approach in order to obtain a numerical solution to the SIR RDE model. Let z be a random variable in $L^2_{\mathbf{P}}$ with a probability density function $\rho(z)$; i.e.,

$$\mathbf{E}\left[z^2\right] = \int |z|^2 \rho(z)\ dz < \infty.$$

We consider the gPC basis functions, $\{\ \Phi_i(z)\ \}$, which are orthogonal polynomial functions such that for $i, j = 0, 1, 2, \cdots$

$$\mathbf{E}\left[\Phi_i(z) \cdot \Phi_j(z)\right] = \nu_i \delta_{ij} \tag{9}$$

where $\nu_i = \mathbf{E}\left[|\Phi_i(z)|^2\right]$ and δ_{ij} is the Kronecker delta function. The type of orthogonal polynomials can be chosen according to the type of distribution for the random variable. For example, if the random variable has a uniform random variable in $[a, b]$, the Legendre polynomials can be used as basis functions satisfying orthogonality (9). In addition, it is best to choose the Jacobi, Hermite, and Laguerre polynomials as basis functions when the random variable has beta, normal, and gamma distributions, respectively. A more general approach, such as arbitrary polynomial chaos (aPC), is used where there is a dependency between random variables [29].

We now derive a high-dimensional ODE system that approximates our model RDE (2) by using gPC. To begin, we apply polynomial chaos expansion to the susceptible compartment $S(t,z)$, the infectious compartment $I(t,z)$, and transmission rate $\beta(z)$:

$$S(t,z)=\sum_{i=0}^{\infty}\tilde{S}_i(t)\Phi_i(z),\ I(t,z)=\sum_{i=0}^{\infty}\tilde{I}_i(t)\Phi_i(z),\ \text{ and }\ \beta(z)=\sum_{i=0}^{\infty}\beta_i\Phi_i(z). \tag{10}$$

Substituting expansions (10) into the SIR RDE (2) gives

$$\begin{aligned}\sum_{i=0}^{\infty}\dot{\tilde{S}}_i(t)\Phi_i(z) &= -\left(\sum_{i=0}^{\infty}\beta_i\Phi_i(z)\right)\left(\sum_{i=0}^{\infty}\tilde{S}_i(t)\Phi_i(z)\right)\left(\sum_{i=0}^{\infty}\tilde{I}_i(t)\Phi_i(z)\right)\\ &\quad -\mu u(t)\left(\sum_{i=0}^{\infty}\tilde{S}_i(t)\Phi_i(z)\right)\\ \sum_{i=0}^{\infty}\dot{\tilde{I}}_i(t)\Phi_i(z) &= \left(\sum_{i=0}^{\infty}\beta_i\Phi_i(z)\right)\left(\sum_{i=0}^{\infty}\tilde{S}_i(t)\Phi_i(z)\right)\left(\sum_{i=0}^{\infty}\tilde{I}_i(t)\Phi_i(z)\right)\\ &\quad -\gamma\left(\sum_{i=0}^{\infty}\tilde{I}_i(t)\Phi_i(z)\right).\end{aligned}$$

Multiplying by $\Phi_\ell(z)$ for $\ell=0,1,\cdots,N$, taking an expectation of the random variable, and truncating the expansions, we have

$$\begin{aligned}\dot{\tilde{S}}_\ell(t) &= -\mathbf{E}\left[\left(\sum_{i=0}^{N}\beta_i\Phi_i(z)\right)\left(\sum_{i=0}^{N}\tilde{S}_i(t)\Phi_i(z)\right)\left(\sum_{i=0}^{N}\tilde{I}_i(t)\Phi_\ell(z)\right)\cdot\Phi_\ell\right]-\mu u(t)\tilde{S}_\ell(t)\\ \dot{\tilde{I}}_\ell(t) &= \mathbf{E}\left[\left(\sum_{i=0}^{N}\beta_i\Phi_i(z)\right)\left(\sum_{i=0}^{N}\tilde{S}_i(t)\Phi_i(z)\right)\left(\sum_{i=0}^{N}\tilde{I}_i(t)\Phi_\ell(z)\right)\cdot\Phi_\ell\right]-\gamma\tilde{I}_\ell(t).\end{aligned} \tag{11}$$

After rearranging (11), we finally obtain a $2(N+1)$-dimensional ODE system that approximates RDE system (2) as follows: for $\ell=0,1,\cdots,N$,

$$\begin{cases}\dot{\tilde{S}}_\ell(t) &= -\displaystyle\sum_{i,j,k=0}^{N}\beta_i\tilde{S}_j(t)\tilde{I}_k(t)\mathbf{E}\left[\Phi_i\cdot\Phi_j\cdot\Phi_k\cdot\Phi_\ell\right]-\mu u(t)\tilde{S}_\ell(t),\\ \dot{\tilde{I}}_\ell(t) &= \displaystyle\sum_{i,j,k=0}^{N}\beta_i\tilde{S}_j(t)\tilde{I}_k(t)\mathbf{E}\left[\Phi_i\cdot\Phi_j\cdot\Phi_k\cdot\Phi_\ell\right]-\gamma\tilde{I}_\ell(t),\end{cases} \tag{12}$$

with initial conditions $\tilde{S}_\ell(0)=\mathbf{E}\left[S_0(z)\Phi_\ell(z)\right]$ and $\tilde{I}_\ell(0)=\mathbf{E}\left[I_0\Phi_\ell(z)\right]$. We use `chaospy`, Python software package [10], to generate orthonormal polynomials $\{\Phi_i\}$ and to compute $\mathbf{E}\left[\Phi_i\cdot\Phi_j\cdot\Phi_k\cdot\Phi_\ell\right]$.

4. Numerical solution to the SIR RDE model

In numerical simulations for the approximate solution to RDE (2), we use the following initial values and parameter values related to the 2009 H1N1 pandemic [4, 11]:

$$\begin{aligned}&N_{tot}=1.155\times10^8,\quad I_0=5\times10^3,\quad S_0=N_{tot}-I_0,\\ &R_0=1.58,\quad \tfrac{1}{\gamma}=1.91,\quad \beta=\tfrac{R_0}{\gamma S_0},\quad \mu=0.7.\end{aligned} \tag{13}$$

4.1. Uniform distribution. In this subsection, we set the random inputs as follows:

$$\beta(z) = \beta_0 + \sigma_\beta \cdot z_1 \quad \text{and} \quad S_0(z) = S_{0,0} + \sigma_{S_0} \cdot z_2,$$

where

$$\beta_0 = 0.95\beta, \quad S_{0,0} = 0.95S_0, \quad \sigma_\beta = 0.1\beta, \quad \text{and} \quad \sigma_{S_0} = 0.1S_0.$$

It is assumed that random variables z_1 and z_2 have a uniform distribution within $[0, 1]$, so $\beta(z) \in [0.95\beta, 1.05\beta]$ and $S_0(z) \in [0.95S_0, 1.05S_0]$. While there are several types of basis functions for the expansions (10) in the polynomial chaos approach, it is best to choose the Legendre polynomials in this case. The first six Legendre polynomials up to the second order used in this numerical simulation are given by

$$\begin{aligned}
\Phi_0(z) &= 1.0 \\
\Phi_1(z) &= 3.46 \cdot z_2 - 1.73 \\
\Phi_2(z) &= 3.46 \cdot z_1 - 1.73 \\
\Phi_3(z) &= 13.41 \cdot z_2^2 - 13.41 \cdot z_2 + 2.23 \\
\Phi_4(z) &= 12.0 \cdot z_1 \cdot z_2 + 1.5 \cdot 10^{-14} \cdot z_2^2 - 6.0 \cdot z_1 - 6.0 \cdot z_2 + 3.0 \\
\Phi_5(z) &= 13.41 \cdot z_1^2 + 1.34 \cdot 10^{-14} \cdot z_1 \cdot z_2 + 1.67 \cdot 10^{-29} \cdot z_2^2 - 13.41 \cdot z_1 \\
&\quad - 6.70 \cdot 10^{-15} \cdot z_2 + 2.24.
\end{aligned}$$

Using `numpy` numerical solver, we obtain $\tilde{S}_i(t)$ and $\tilde{I}_i(t)$ by solving high-dimensional ODE system (12). In Figure 1, we present a density of realizations by Monte-Carlo simulation, the average values of Monte-Carlo results (black solid line), and the expectation values of the approximate solutions (black dashed line), i.e., $\mathbf{E}\left[\sum_{i=0}^{N} \tilde{S}_i(t)\Phi_i(z)\right]$ and $\mathbf{E}\left[\sum_{i=0}^{N} \tilde{I}_i(t)\Phi_i(z)\right]$, for comparison. In the Monte-Carlo simulation, we solve equation (2) using 1,000 samples for $\beta(z)$ and $S_0(z)$ generated by the uniform distribution. As depicted in Figure 1, the results using the Monte-Carlo method and the gPC approach are nearly identical. Figure 2 shows the histograms of $\beta(z)$ and $S_0(z)$. The data shown is a random sample of 1,000 points from a uniform distribution $[0, 1]$, i.e., $z_i \sim U(0, 1)$. In Figure 3, we explore the effect of the order in the basis polynomial by presenting the distributions of approximate solutions $S(t, z)$ and $I(t, z)$ for different orders of basis polynomial ($d = 1, 2, 3$, and 4) at time $t = 20$ and 60. We can see that the distributions of the solutions with a polynomial order of 2 or more are similar to the distribution obtained by Monte-Carlo simulation.

4.2. Normal distribution. In this section, we examine the results of the Monte-Carlo simulation and gPC approximation with random inputs $\beta(z)$ and $S_0(z)$ where z is a random vector with a two-dimensional independent normal distribution. We set the random inputs as follows:

$$\beta(z) = \beta_0 + \sigma_\beta \cdot z_1 \quad \text{and} \quad S_0(z) = S_{0,0} + \sigma_{S_0} \cdot z_2,$$

where

$$\beta_0 = \beta, \quad S_{0,0} = S_0, \quad \sigma_\beta = \frac{0.05\beta}{3}, \quad \text{and} \quad \sigma_{S_0} = \frac{0.05S_0}{3}.$$

It is assumed that random variables z_1 and z_2 have a normal distribution with mean 0 and a standard deviation of 1, i.e., $z_i \sim N(0, 1)$, for $i = 1, 2$. So the 3σ intervals of $\beta(z)$ and $S_0(z)$ are $[0.95\beta, 1.05\beta]$ and $[0.95S_0, 1.05S_0]$, respectively.

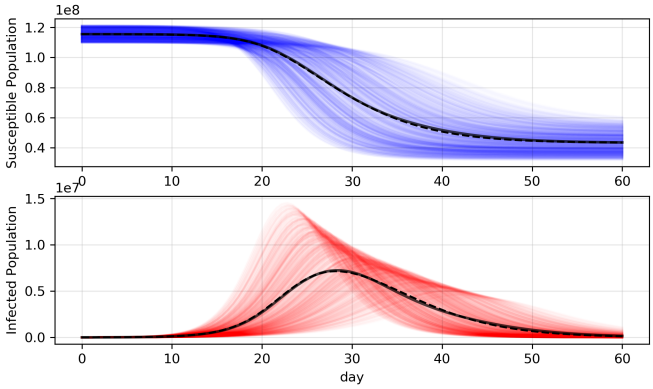

FIGURE 1. The density of realizations for $S(t,z)$ and $I(t,z)$ with 1,000 samples from a Monte-Carlo simulation when the random variables have a uniform distribution. The bold solid line represents the average values of the Monte-Carlo results and the bold dashed line represents the expectation values of the approximate solutions from gPC.

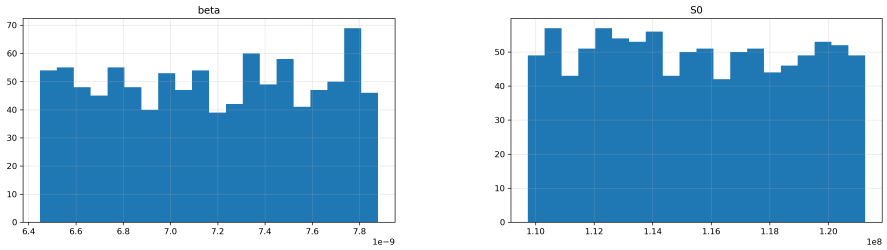

(A) Histogram of $\beta(z)$ (B) Histogram of $S_0(z)$

FIGURE 2. 1,000 samples of $\beta(z)$ and $S_0(z)$ where $z = (z_1, z_2)$ such that $z_i \sim U(0,1)$.

In the normal distribution, the Hermite polynomial could be chosen as a basis function for gPC expansion. The normalized Hermite polynomials up to the second order are given by

$$\begin{aligned}
\Phi_0(z) &= 1.0 \\
\Phi_1(z) &= z_2 \\
\Phi_2(z) &= z_1 \\
\Phi_3(z) &= 0.71 \cdot z_2^2 - 0.71 \\
\Phi_4(z) &= z_1 \cdot z_2 \\
\Phi_5(z) &= 0.71 \cdot z_1^2 - 0.71.
\end{aligned}$$

As shown in Figure 4, 5, and 6, most of the numerical results from Monte-Carlo simulation and the gPC approach are similar to those in Subsection 4.1. The

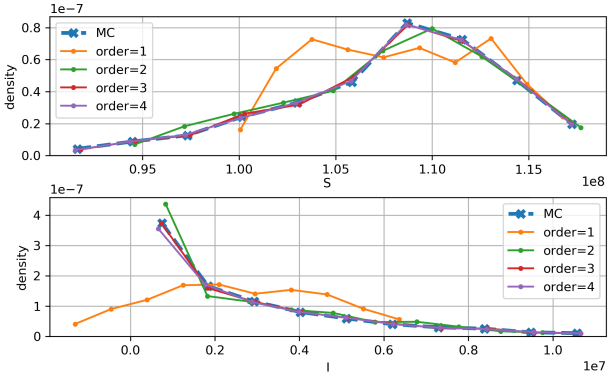

(A) $t = 20$

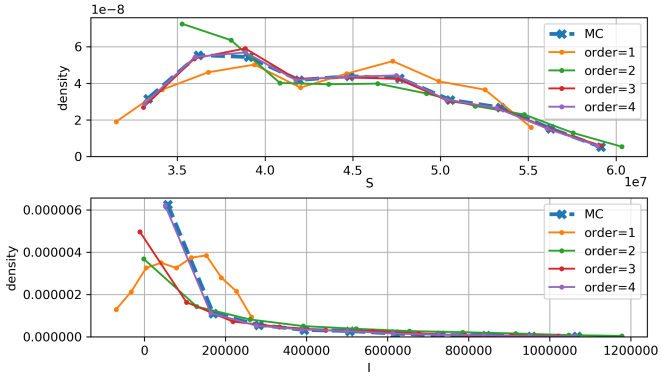

(B) $t = 60$

FIGURE 3. Distributions of approximate solutions $S(t, z)$ and $I(t, z)$ for different orders of the basis polynomial ($d = 1, 2, 3$, and 4) from gPC at time $t = 20$ and 60 when the random variables have a uniform distribution. The blue cross marker represents the results from the Monte-Carlo simulation.

only difference is that the approximations for the distribution of infectious solution $I(t, z)$ are not good for odd-order cases in Figure 6.

5. Optimal control of the SIR RDE model

The main goal of this study is to design an efficient vaccination strategy for influenza outbreaks using the SIR RDE model. One way to achieve this goal is to explore an optimal control problem that minimizes not only the mean number of infected people, but also the cost of vaccination. Thus, we define the objective or cost functional as

$$\mathcal{J}(u, S, I) = \mathbf{E} \int_0^T w_1 I^2(t, z) + w_2 u S(t, z) + w_3 u^2(t)\, dt. \tag{14}$$

The second and third terms in the objective functional represent the number of vaccines administered and the cost related to vaccination, respectively, while w_1,

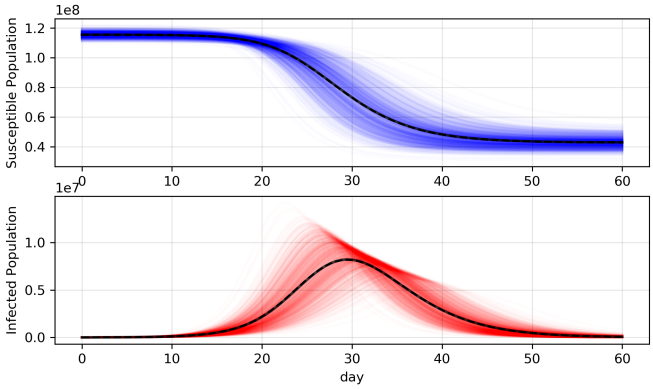

FIGURE 4. The density of realizations for $S(t,z)$ and $I(t,z)$ with 1,000 samples from Monte-Carlo simulation when the random variables have a normal distribution. The bold solid line represents the average values of the Monte-Carlo results and the bold dashed line represents the expectation values of the approximate solutions from gPC.

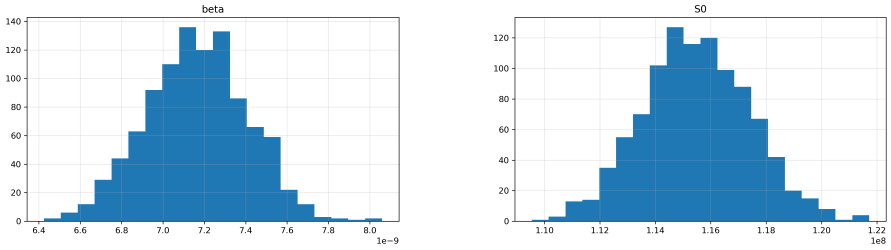

(A) Histogram of $\beta(z)$ (B) Histogram of $S_0(z)$

FIGURE 5. 1,000 samples of $\beta(z)$ and $S_0(z)$ where $z = (z_1, z_2)$ such that $z_i \sim N(0,1)$.

w_2, and w_3 are weight constants to balance the relative costs in the objective functional (14). The weight constants can also be chosen to change the relative importance of each term in the functional. Let $\mathcal{U}$ be the set of admissible control functions:

$$\mathcal{U} = L^\infty([0,T];U) \quad \text{where} \quad U = [0,1].$$

Now our optimal control problem can be formulated as

$$\text{(OP)} \qquad \min_{u\in\mathcal{U}} \mathcal{J}(u,S,I) \text{ subject to the SIR RDE model (2).}$$

To compute the optimal control function associated with problem (OP), we should derive an optimality system which is the necessary conditions of the optimal solution of the problem. However, it is not easy to derive the optimality system, because constraint equations (2) are random differential equations. We use the gPC approach to overcome this difficulty. The gPC approach converts the optimal control problem of random differential equations into an optimal control

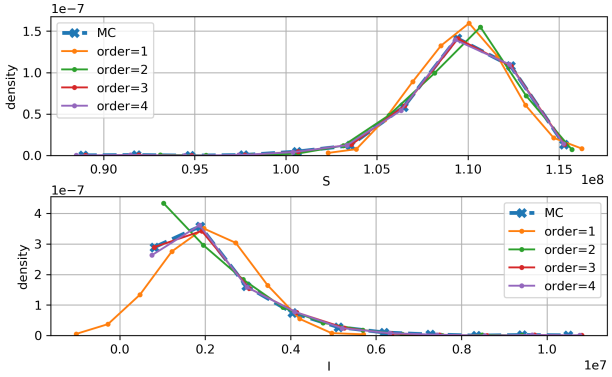

(A) $t = 20$

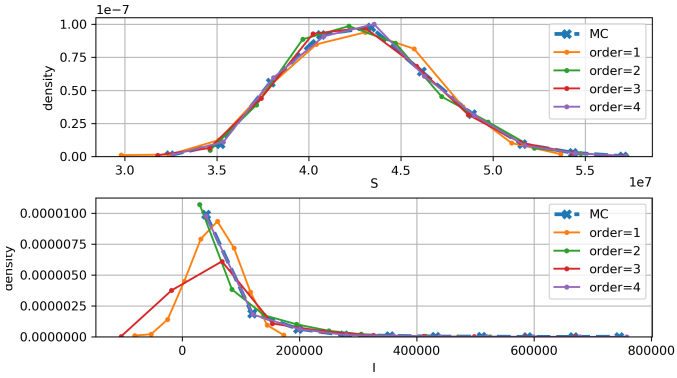

(B) $t = 60$

FIGURE 6. Distributions of approximate solution $S(t, z)$ and $I(t, z)$ for different orders of basis polynomial ($d = 1, 2, 3$, and 4) from gPC at time $t = 20$ and 60 when the random variables have a normal distribution. The blue cross marker represents the results from Monte-Carlo simulation.

problem of high-dimensional ordinary differential equations by applying polynomial chaos expansion. The original optimal control problem (OP) is transformed into approximate optimal control problem (AOP) as follows: for fixed N,

(AOP) $\min_{u \in \mathcal{U}} \mathcal{J}(u, \tilde{S}, \tilde{I})$ subject to the high-dimensional SIR ODE system (12)

where $\tilde{S} = \sum_{i=0}^{N} \tilde{S}_i(t)\Phi_i(z)$ and $\tilde{I} = \sum_{i=0}^{N} \tilde{I}_i(t)\Phi_i(z)$ are the solution to high-dimensional SIR ODE system (12).

We now derive an optimality system that characterizes the optimal control function by using Pontryagin's Maximum Principle [6]. The system can be used to compute candidates for optimal controls. For this, we first introduce a Hamiltonian that consists of the integrand of objective functional (14), coupled with the

right-hand sides of high-dimensional SIR ODE system (12) through adjoint variables $\lambda_{\tilde{S}_n}(t)$ and $\lambda_{\tilde{I}_n}(t)$ for $n = 0, 1, 2, \cdots, N$. Since our control function is bounded, we define Lagrangian (L) which is the Hamiltonian augmented with penalty terms for boundedness. Before defining the Lagrangian, we need to rewrite objective functional (14) for simplicity:

$$\begin{aligned}
&\mathbf{E}\int_0^T w_1\tilde{I}^2(t,z) + w_2 u\tilde{S}(t,z) + w_3 u^2(t)\ dt \\
&\quad = \int_0^T w_1 \mathbf{E}\left[\left(\sum_{i=0}^N \tilde{I}_i(t)\Phi_i(z)\right)^2\right] + w_2 u\mathbf{E}\left[\sum_{i=0}^N \tilde{S}_i(t)\Phi_i(z)\right] + w_3 u^2(t)\ dt \\
&\quad = \int_0^T w_1 \sum_{i=0}^N \tilde{I}_i^2(t) + w_2 u\tilde{S}_0(t) + w_3 u^2(t)\ dt
\end{aligned}$$

Lagrangian (L) is now defined by

$$\begin{aligned}
L = {} & w_1 \sum_{i=0}^N \tilde{I}_i^2 + w_2 u(t)\tilde{S}_0 + w_3 u^2(t) \\
& + \sum_{\ell=0}^N \lambda_{\tilde{S}_\ell}\left(-\sum_{i,j,k=0}^N \beta_i \tilde{S}_j(t)\tilde{I}_k(t)\mathbf{E}\left[\Phi_i\cdot\Phi_j\cdot\Phi_k\cdot\Phi_\ell\right] - \mu u(t)\tilde{S}_\ell(t)\right) \\
& + \sum_{\ell=0}^N \lambda_{\tilde{I}_\ell}\left(\sum_{i,j,k=0}^N \beta_i \tilde{S}_j(t)\tilde{I}_k(t)\mathbf{E}\left[\Phi_i\cdot\Phi_j\cdot\Phi_k\cdot\Phi_\ell\right] - \gamma\tilde{I}_\ell(t)\right) \\
& - v_1(t)u(t) - v_2(t)(1-u(t)),
\end{aligned}$$

where $v_i(t) \geq 0$, $(i = 1, 2)$ are the penalty multipliers satisfying

$$v_1(t)u(t) = v_2(t)(1-u(t)) = 0 \quad \text{at} \quad u = u^*. \tag{15}$$

Here u^* is the optimal control function yet to be found.

Theorem 5.1. *Given optimal control function u^* and the corresponding solutions $(\tilde{S}, \tilde{I})$ to high-dimensional SIR ODE system* (12) *that minimize objective functional* (14)*, there exist adjoint variables $\lambda_{\tilde{S}_n}(t)$ and $\lambda_{\tilde{I}_n}(t)$ for $n = 0, 1, 2, \cdots, N$ satisfying* (16)

$$\begin{aligned}
\dot{\lambda}_{\tilde{S}_n} &= -w_2 u\delta_{0n} - \lambda_{\tilde{S}_n}\left(-\sum_{i,k=0}^N \beta_i \tilde{I}_k E_{inkn} - \mu u(t)\right) - \lambda_{\tilde{I}_n}\left(\sum_{i,k=0}^N \beta_i \tilde{I}_k E_{inkn}\right) \\
\dot{\lambda}_{\tilde{I}_n} &= -2w_1\tilde{I}_n - \lambda_{\tilde{S}_n}\left(-\sum_{i,j=0}^N \beta_i \tilde{S}_j E_{ijnn}\right) - \lambda_{\tilde{I}_n}\left(\sum_{i,j=0}^N \beta_i \tilde{S}_j E_{ijnn} - \gamma\right)
\end{aligned}$$

with terminal conditions $\lambda_{\tilde{S}_n}(T) = \lambda_{\tilde{I}_n}(T) = 0$ where

$$E_{ijk\ell} = \mathbf{E}\left[\Phi_i\cdot\Phi_j\cdot\Phi_k\cdot\Phi_\ell\right].$$

Moreover, optimal control u^* is characterized as

$$u^*(t) = \max\left(0, \min\left(1, \frac{1}{2w_3}\left[\mu\sum_{\ell=0}^N \lambda_{\tilde{S}_\ell}(t)\tilde{S}_\ell(t) - w_2\tilde{S}_0\right]\right)\right). \tag{17}$$

Proof. The results follow from an application of Pontryagin's Maximum Principle [6]. Differentiating Lagrangian L with respect to state variables $\tilde{S}_n$ and $\tilde{I}_n$, respectively, we obtain the equations for adjoint variables $\lambda_{\tilde{S}_n}(t)$ and $\lambda_{\tilde{I}_n}(t)$ as follows for $n = 0, 1, 2, \cdots, N$:

$$\begin{aligned}
\dot{\lambda}_{\tilde{S}_n} = -\frac{\partial H}{\partial \tilde{S}_n} &= -w_2 u\delta_{0n} - \sum_{\ell=0}^{N} \lambda_{\tilde{S}_\ell} \left(- \sum_{i,j,k=0}^{N} \beta_i \delta_{jn} \tilde{I}_k E_{ijk\ell} - \mu u(t) \delta_{\ell n} \right) \\
&\quad - \sum_{\ell=0}^{N} \lambda_{\tilde{I}_\ell} \left(\sum_{i,j,k=0}^{N} \beta_i \delta_{jn} \tilde{I}_k E_{ijk\ell} \right) \\
&= -w_2 u\delta_{0n} + \lambda_{\tilde{S}_n} \left(\sum_{i,k=0}^{N} \beta_i \tilde{I}_k E_{inkn} + \mu u(t) \right) - \lambda_{\tilde{I}_n} \left(\sum_{i,k=0}^{N} \beta_i \tilde{I}_k E_{inkn} \right) \\
\dot{\lambda}_{\tilde{I}_n} = -\frac{\partial H}{\partial \tilde{I}_n} &= -2w_1 \tilde{I}_n - \sum_{\ell=0}^{N} \lambda_{\tilde{S}_\ell} \left(- \sum_{i,j,k=0}^{N} \beta_i \tilde{S}_j \delta_{kn} E_{ijk\ell} \right) \\
&\quad - \sum_{\ell=0}^{N} \lambda_{\tilde{I}_\ell} \left(\sum_{i,j,k=0}^{N} \beta_i \tilde{S}_j \delta_{kn} E_{ijk\ell} - \gamma \delta_{\ell n} \right) \\
&= -2w_1 \tilde{I}_n - \lambda_{\tilde{S}_n} \left(- \sum_{i,j=0}^{N} \beta_i \tilde{S}_j E_{ijnn} \right) - \lambda_{\tilde{I}_n} \left(\sum_{i,j=0}^{N} \beta_i \tilde{S}_j E_{ijnn} - \gamma \right)
\end{aligned}$$

with terminal conditions $\lambda_{\tilde{S}_n}(T) = \lambda_{\tilde{I}_n}(T) = 0$ where

$$E_{ijk\ell} = \mathbf{E}\left[\Phi_i \cdot \Phi_j \cdot \Phi_k \cdot \Phi_\ell\right].$$

To obtain the formulation of optimal control function u^*, we investigate necessary optimality condition $\frac{\partial L}{\partial u} = 0$; that is,

$$\frac{\partial L}{\partial u} = w_2 \tilde{S}_0 + 2w_3 u - \mu \sum_{\ell=0}^{N} \lambda_{\tilde{S}_\ell} \tilde{S}_\ell - v_1 + v_2 = 0. \tag{18}$$

Solving for optimal control u^* we have

$$u^* = \frac{1}{2w_3} \left[\mu \sum_{\ell=0}^{N} \lambda_{\tilde{S}_\ell} \tilde{S}_\ell - w_2 \tilde{S}_0 + v_1 - v_2 \right].$$

To obtain an explicit formula for optimal control without penalty multipliers v_1 and v_2, we consider the following three cases:

1. In the set $\{t | 0 < u^*(t) < 1\}$, we have $v_1(t) = v_2(t) = 0$ because of the condition for penalty multipliers (15). Hence, optimal control is given by

$$u^* = \frac{1}{2w_3} \left[\mu \sum_{\ell=0}^{N} \lambda_{\tilde{S}_\ell} \tilde{S}_\ell - w_2 \tilde{S}_0 \right].$$

2. In the set $\{t | u^*(t) = 1\}$, we have $v_1(t) = 0$ because of the condition for penalty multipliers (15). Hence,

$$1 = u^* = \frac{1}{2w_3} \left[\mu \sum_{\ell=0}^{N} \lambda_{\tilde{S}_\ell} \tilde{S}_\ell - w_2 \tilde{S}_0 - v_2 \right],$$

which implies that

$$\frac{1}{2w_3}\left[\mu\sum_{\ell=0}^{N}\lambda_{\tilde{S}_\ell}\tilde{S}_\ell - w_2\tilde{S}_0\right] \geq 1,$$

since $v_2 \geq 0$.

3. In the set $\{t|u^*(t) = 0\}$, we have $v_2(t) = 0$ because of the condition for penalty multipliers (15). Hence,

$$0 = u^* = \frac{1}{2w_3}\left[\mu\sum_{\ell=0}^{N}\lambda_{\tilde{S}_\ell}\tilde{S}_\ell - w_2\tilde{S}_0 + v_1\right],$$

which implies that

$$\frac{1}{2w_3}\left[\mu\sum_{\ell=0}^{N}\lambda_{\tilde{S}_\ell}\tilde{S}_\ell - w_2\tilde{S}_0\right] \leq 0,$$

since $v_1 \geq 0$.

Combining these three cases, we finally obtain the explicit formula for u^* (17). □

Remark 5.2. *The system consisting of the state system* (12) *with initial conditions, the adjoint system* (16) *with terminal conditions, and the optimality condition* (17) *is called the optimality system (AOP) for fixed N. Any optimal controls must satisfy this system.*

6. Numerical results

In this section, we describe a numerical algorithm for determining a solution to approximate optimal control problem (AOP). We point out that the optimality system is a two-point boundary value problem because initial conditions are specified for state system (12), whereas terminal conditions are specified for adjoint system (16). Among many practical approaches to solving the two-point boundary value problem, we use a gradient-type iterative method. The algorithm proceeds as follows.

- Randomly choose an initial guess for control.
- Solve state system (12) forward in time by using the control.
- Solve adjoint system (16) backward in time.
- Update the control by using optimality condition (17).
- Continue the iterations until convergence is achieved.

For more information on the gradient method, we refer interested readers to [13]. In numerical simulations, the weight constants are selected as $w_1 = w_2 = 1$ and $w_3 = 10^7$, and the degree of the orthonormal polynomial is $d = 2$. The rest of the parameters are the same as they are in (13). We simulate optimal vaccination strategies for a 60-day period, with various distributions of random variables z_1 and z_2.

Figure 7 shows the optimal vaccination strategy and the 1,000 sample paths of corresponding states S and I with a uniform distribution ($z_i \sim U(0, 1)$). As depicted in Figure 7 (a), the optimal strategy indicates that in the first few days, vaccination should be given at the highest rate, and after that, vaccination should be stopped completely. In Figure 7 (b) and (c), we present the 1,000 sample paths of the SIR RDE model with an optimal vaccination strategy and without vaccination, respectively, for comparison purposes. Compared with no vaccination, we can see that the number of infected individuals is well-controlled, and the range of variation in the 1,000 sample paths for S and I is significantly reduced under the

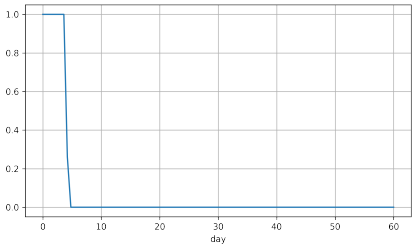

(A) Optimal control function.

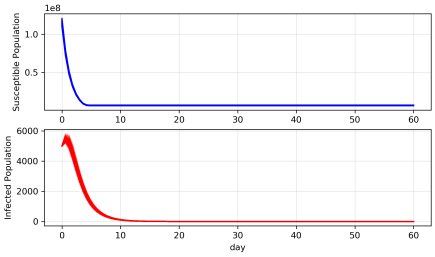

(B) 1,000 sample paths of S and I with the optimal vaccination.

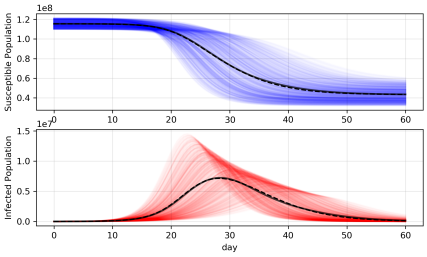

(C) 1,000 sample paths of S and I without vaccination.

FIGURE 7. Optimal control and dynamics of the RDE SIR model with a uniform distribution.

optimal vaccination strategy. This means that the optimal vaccination strategy not only effectively controls infectious diseases, but also mitigates, to some extent, the uncertainty arising in the real world.

We explore how the distribution type of random variables affects the optimal vaccination strategy. Figure 8, 9, and 11, shows the optimal vaccination strategies and the 1,000 sample paths of corresponding states S and I with a normal distribution ($z_i \sim N(0,1)$), a beta distribution ($z_i \sim B(0.5,0.5)$), and a gamma distribution ($z_i \sim \Gamma(9,0.5)$), respectively. Observe that the overall results are similar to the case with a uniform distribution. This means that vaccination strategies are insensitive to uncertainties that depend on measurement methods and errors, on differences in the actual population sample sizes used, and on other factors that are difficult to account for.

Figure 10 and 12 show the histograms of $\beta(z)$ and $S_0(z)$ with a beta distribution and a gamma distribution, respectively. With the beta distribution, we set the random parameters as follows:

$$\beta(z) = \beta_0 + \sigma_\beta \cdot z_1 \quad \text{and} \quad S_0(z) = S_{0,0} + \sigma_{S_0} \cdot z_2,$$

where

$$\beta_0 = 0.95\beta, \quad S_{0,0} = 0.95S_0, \quad \sigma_\beta = 0.1\beta, \quad \text{and} \quad \sigma_{S_0} = 0.1S_0.$$

It is assumed that random variables z_1 and z_2 have a beta distribution, $B(0.5,0.5)$ in $[0,1]$, so then, $\beta(z) \in [0.95\beta, 1.05\beta]$, and $S_0(z) \in [0.95S_0, 1.05S_0]$. And the

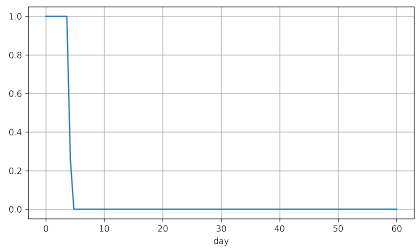

(A) Optimal control function.

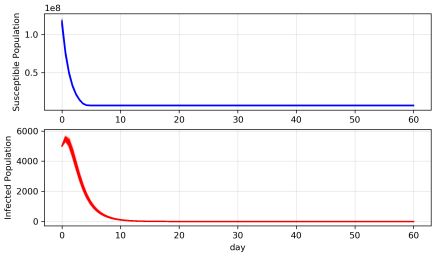

(B) 1,000 sample paths of S and I with the optimal vaccination.

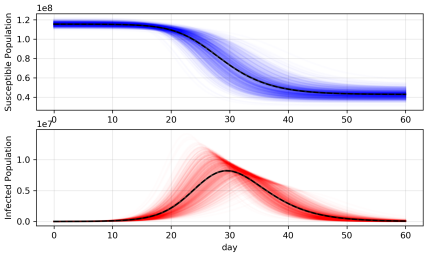

(C) 1,000 sample paths of S and I without vaccination.

FIGURE 8. Optimal control and dynamics of the RDE SIR model with a normal distribution.

orthonormal basis polynomials $\{\Phi_i\}$ up to the second order are given by

$$\begin{aligned}
\Phi_0(z) &= 1.0 \\
\Phi_1(z) &= 2.83 \cdot z_2 - 1.41 \\
\Phi_2(z) &= 2.83 \cdot z_1 - 1.41 \\
\Phi_3(z) &= 11.31 \cdot z_2^2 - 11.31 \cdot z_2 + 1.41 \\
\Phi_4(z) &= 8.0 \cdot z_1 \cdot z_2 - 4.0 \cdot z_1 - 4l0 \cdot z_2 + 2.0 \\
\Phi_5(z) &= 11.31 \cdot z_1^2 - 11.31 \cdot z_1 + 1.41.
\end{aligned}$$

With the gamma distribution, the random inputs are defined by

$$\beta(z) = \beta_0 + \sigma_\beta \cdot z_1 \quad \text{and} \quad S_0(z) = S_{0,0} + \sigma_{S_0} \cdot z_2,$$

where

$$\beta_0 = 0.95\beta, \quad S_{0,0} = 0.95S_0, \quad \sigma_\beta = 0.1\beta/10, \quad \text{and} \quad \sigma_{S_0} = 0.1S_0/10.$$

It is assumed that random variables z_1 and z_2 have a gamma distribution, $\Gamma(9, 0.5)$ in $[0, 1]$, so then, $\beta(z) \in [0.95\beta, 1.05\beta]$, and $S_0(z) \in [0.95S_0, 1.05S_0]$. And the

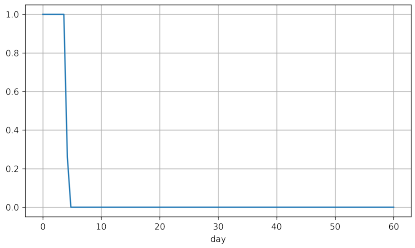

(A) Optimal control function.

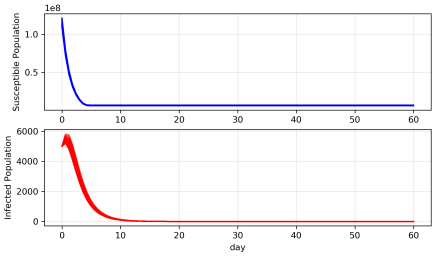

(B) 1,000 sample paths of S and I with the optimal vaccination.

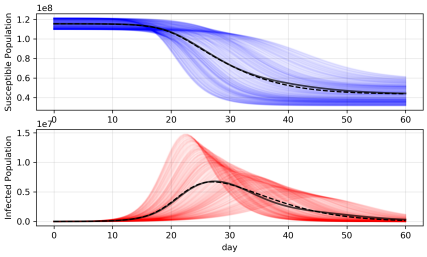

(C) 1,000 sample paths of S and I without vaccination.

FIGURE 9. Optimal control and dynamics of the RDE SIR model with a beta distribution.

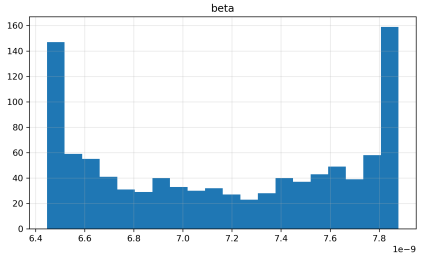

(A) Histogram of $\beta(z)$

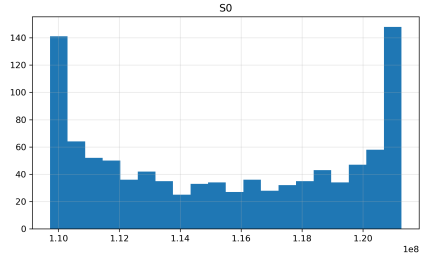

(B) Histogram of $S_0(z)$

FIGURE 10. 1,000 samples of $\beta(z)$ and $S_0(z)$ where $z = (z_1, z_2)$ such that $z_i \sim B(0.5, 0.5)$.

orthonormal basis polynomials for a gamma distribution are as follows:

$$\Phi_0(z) = 1.0$$
$$\Phi_1(z) = 0.67 \cdot z_2 - 3.0$$
$$\Phi_2(z) = 0.67 \cdot z_1 - 3.0$$
$$\Phi_3(z) = 0.30 \cdot z_2^2 - 2.99 \cdot z_2 + 6.70$$
$$\Phi_4(z) = 0.44 \cdot z_1 \cdot z_2 - 2.0 \cdot z_1 - 2.0 \cdot z_2 + 9.0$$
$$\Phi_5(z) = 0.30 \cdot z_1^2 - 2.99 \cdot z_1 + 6.70.$$

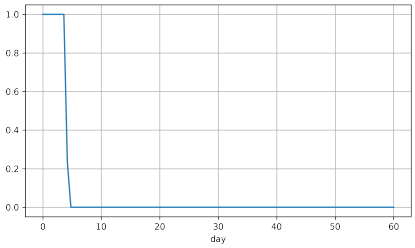

(A) Optimal control function.

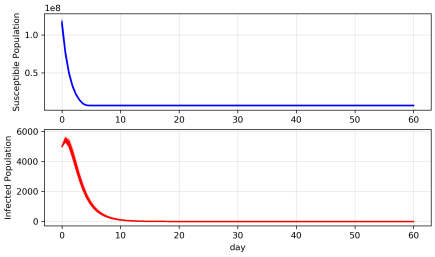

(B) 1,000 sample paths of S and I with the optimal vaccination.

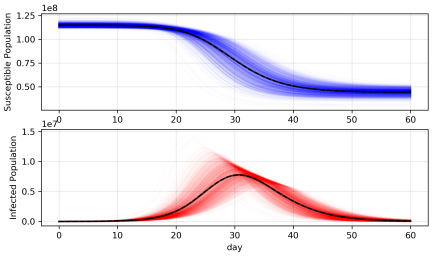

(C) 1,000 sample paths of S and I without vaccination.

FIGURE 11. Optimal control and dynamics of the RDE SIR model with a gamma distribution.

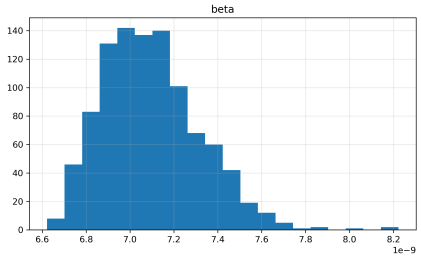

(A) Histogram of $\beta(z)$

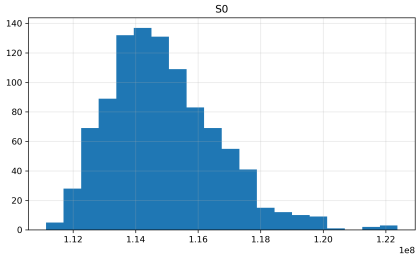

(B) Histogram of $S_0(z)$

FIGURE 12. 1,000 samples of $\beta(z)$ and $S_0(z)$ where $z = (z_1, z_2)$ such that $z_i \sim \Gamma(9, 0.5)$.

7. Conclusion

We presented the generalized polynomial chaos Galerkin method to solve an optimal control problem of the SIR epidemic model with random inputs. The gPC expansion and the stochastic Galerkin procedure allow us to employ standard numerical techniques and control theory by converting the RDE to a system of ODEs. The solution of the SIR RDE obtained by the gPC Galerkin method was compared by using Monte-Carlo simulations to verify accuracy. A low-degree gPC

provides a reasonable estimate of the mean, but a higher order basis is required for good approximation of complete distributions of the state variables.

Pontryagin's principle was used to derive an optimality system from which the optimal control was determined. While the perturbations of inputs greatly vary the dynamics without vaccination, optimal control and the resulting states are very robust to the uncertainty of parameters β and S_0. In addition, the optimal vaccination strategies suggested from simulations are similar to each other regardless of the type of distributions for the random inputs. As a result, the deterministic SIR model can be a simple and acceptable alternative if the optimal solution is one's only concern.

In this study, we considered the source of uncertainties which were independent of each other for the SIR model. The proposed approach can be extended to a more practical problem assuming a correlated random source such as a multinormal distribution with non-zero covariance or an arbitrary distribution. For this extension, more generalized tools to represent the random variables, for example arbitrary polynomial chaos, are needed [29]. We may also apply the proposed scheme to various disease models with random inputs other than the SIR model. HIV [1, 15] is an interesting example for investigating the impact of randomness, and to design individual therapy regimens, because the experimental data exhibit significant variability among patients and their responses to therapy.

Acknowledgements

The work of Hee-Dae Kwon was supported by NRF-2016R1D1A1B04931897 and NRF-2021R1A2C1009878. The work of Jeehyun Lee was supported by a government-wide R&D fund project for infectious disease research through GFID, seven ministries (grant number: HG20C0003) and 2020R1A2C1A0101077511.

References

[1] BM Adams, HT Banks, M Davidian, Hee-Dae Kwon, HT Tran, SN Wynne, and ES Rosenberg. Hiv dynamics: modeling, data analysis, and optimal treatment protocols. Journal of Computational and Applied Mathematics, 184(1):10–49, 2005.

[2] Julien Arino, Fred Brauer, Pauline Van Den Driessche, James Watmough, and Jianhong Wu. A model for influenza with vaccination and antiviral treatment. Journal of theoretical biology, 253(1):118–130, 2008.

[3] Harvey Thomas Banks, Shuhua Hu, and W Clayton Thompson. Modeling and inverse problems in the presence of uncertainty. CRC Press, 2014.

[4] Matthew Biggerstaff, Simon Cauchemez, Carrie Reed, Manoj Gambhir, and Lyn Finelli. Estimates of the reproduction number for seasonal, pandemic, and zoonotic influenza: a systematic review of the literature. BMC infectious diseases, 14(1):480, 2014.

[5] Kbenesh Blayneh, Yanzhao Cao, and Hee-Dae Kwon. Optimal control of vector-borne diseases: treatment and prevention. Discrete and Continuous Dynamical Systems B, 11(3):587–611, 2009.

[6] VG Boltyanskiy, Revaz V Gamkrelidze, YEF MISHCHENKO, and LS Pontryagin. Mathematical theory of optimal processes. 1962.

[7] Fred Brauer. Some simple epidemic models. Mathematical Biosciences and Engineering, 3(1):1, 2006.

[8] M-C Casabán, J-C Cortés, J-V Romero, and M-D Roselló. Probabilistic solution of random si-type epidemiological models using the random variable transformation technique. Communications in Nonlinear Science and Numerical Simulation, 24(1-3):86–97, 2015.

[9] J. C. Cortés, J. V. Romero, M. D. Roselló, and R. J. Villanueva. Improving adaptive generalized polynomial chaos method to solve nonlinear random differential equations by the random variable transformation technique. Communications in Nonlinear Science and Numerical Simulation, 2017.

[10] Jonathan Feinberg and Hans Petter Langtangen. Chaospy: An open source tool for designing methods of uncertainty quantification. Journal of Computational Science, 11:46–57, 2015.

[11] Christophe Fraser, Christl A Donnelly, Simon Cauchemez, William P Hanage, Maria D Van Kerkhove, T Déirdre Hollingsworth, Jamie Griffin, Rebecca F Baggaley, Helen E Jenkins, Emily J Lyons, et al. Pandemic potential of a strain of influenza a (h1n1): early findings. science, 324(5934):1557–1561, 2009.
[12] A. Friedman. Stochastic Differential Equations and Applications. Dover Books on Mathematics. Dover Publications, 2012.
[13] Max D Gunzburger. Perspectives in flow control and optimization, volume 5. Siam, 2003.
[14] Herbert W Hethcote. The mathematics of infectious diseases. SIAM Review, 42(4):599–653, 2000.
[15] Tae Soo Jang, Jungeun Kim, Hee-Dae Kwon, and Jeehyun Lee. Hybrid on-off controls for an hiv model based on a linear control problem. Journal of the Korean Mathematical Society, 52(3):469–487, 2015.
[16] E. Jung, Suzanne Lenhart, and Z. Feng. Optimal control of treatments in a two-strain tuberculosis model. Discrete and Continuous Dynamical Systems Series B, 2(4):473–482, 2002.
[17] Bonnie Kegan and R. Webster West. Modeling the simple epidemic with deterministic differential equations and random initial conditions. Mathematical Biosciences, 2005.
[18] William Ogilvy Kermack and Anderson G McKendrick. A contribution to the mathematical theory of epidemics. Proceedings of the Royal Society of London. Series A, Containing papers of a mathematical and physical character, 115(772):700–721, 1927.
[19] R Kovacevic. Stochastic SIS Epidemic Models-The PDE-Approach. 2015.
[20] A. Lahrouz, H. El Mahjour, A. Settati, and A. Bernoussi. Dynamics and optimal control of a non-linear epidemic model with relapse and cure. Physica A: Statistical Mechanics and its Applications, 496:299–317, 2018.
[21] Jeehyun Lee, Jungeun Kim, and Hee-Dae Kwon. Optimal control of an influenza model with seasonal forcing and age-dependent transmission rates. Journal of Theoretical Biology, 317:310–320, 2013.
[22] Sunmi Lee and Gerardo Chowell. Exploring optimal control strategies in seasonally varying flu-like epidemics. Journal of Theoretical Biology, 412:36–47, 2017.
[23] Sunmi Lee, Michael Golinski, and Gerardo Chowell. Modeling optimal age-specific vaccination strategies against pandemic influenza. Bulletin of Mathematical Biology, 74(4):958–980, 2012.
[24] Kezan Li, Guanghu Zhu, Zhongjun Ma, and Lijuan Chen. Dynamic stability of an siqs epidemic network and its optimal control. Communications in Nonlinear Science and Numerical Simulation, 66:84–95, 2019.
[25] Yoshihiro Maki and Hideo Hirose. Infectious disease spread analysis using stochastic differential equations for sir model. In 2013 4th International Conference on Intelligent Systems, Modelling and Simulation, pages 152–156. IEEE, 2013.
[26] X. Mao. Stochastic Differential Equations and Their Applications. Ellis Horwood series in mathematics and its applications. Horwood Pub., 1997.
[27] Bernt Oksendal. Stochastic Differential Equations. An Introduction with Applications. Springer Science & Business Media, Berlin, Heidelberg, March 2013.
[28] Almbrok Hussin Alsonosi Omar and Yahya Abu Hasan. Numerical simulations of an SIR epidemic model with random initial states. ScienceAsia, 39:42–47, 2013.
[29] Joel A Paulson, Edward A Buehler, and Ali Mesbah. Arbitrary polynomial chaos for uncertainty propagation of correlated random variables in dynamic systems. IFAC-PapersOnLine, 50(1):3548–3553, 2017.
[30] Howida Slama, A. Hussein, Nabila A. El-Bedwhey, and Mustafa M. Selim. An approximate probabilistic solution of a random SIR-type epidemiological model using RVT technique. Applied Mathematics and Computation, 2019.
[31] Tsu T Soong. Random differential equations in science and engineering. Elsevier, 1973.
[32] Dongbin Xiu. Numerical Methods for Stochastic Computations. A Spectral Method Approach. Princeton University Press, July 2010.
[33] Dongbin Xiu and Jan S Hesthaven. High-order collocation methods for differential equations with random inputs. SIAM Journal on Scientific Computing, 27(3):1118–1139, 2005.
[34] Tianhu Yu, Dengqing Cao, and Shengqiang Liu. Epidemic model with group mixing: Stability and optimal control based on limited vaccination resources. Communications in Nonlinear Science and Numerical Simulation, 61:54–70, 2018.

Department of Computational Science and Engineering, Yonsei University, 50 Yonsei-ro Seodaemun-gu, Seoul, 03722, Republic of Korea, and Data Analytics & Artificial Intelligence Research Center, LG CNS, Seoul, Republic of Korea
E-mail: yoongu.hwang@gmail.com

Department of Mathematics, Inha University, 100 Inharo Nam-gu, Incheon, 22212, Republic of Korea
E-mail: hdkwon@inha.ac.kr

School of Mathematics and Computing (Mathematics), Yonsei University, 50 Yonsei-ro Seodaemun-gu, Seoul, 03722, Republic of Korea
E-mail: ezhyun@yonsei.ac.kr